Bioorganic & Medicinal Chemistry Letters 20 (2010) 2068–2073

Contents lists available at ScienceDirect

Bioorganic & Medicinal Chemistry Letters

journal homepage: www.elsevier.com/locate/bmcl

# Novel pyrrolyl 2-aminopyridines as potent and selective human β-secretase (BACE1) inhibitors

Michael S. Malamas [a,*], Keith Barnes [b], Yu Hui [b], Matthew Johnson [b], Frank Lovering [a], Jeff Condon [a], William Fobare [a], William Solvibile [a], Jim Turner [c], Yun Hu [c], Eric S. Manas [a,†], Kristi Fan [a], Andrea Olland [d], Rajiv Chopra [d], Jonathan Bard [c], Menelas N. Pangalos [c], Peter Reinhart [c], Albert J. Robichaud [a]

[a] Department of Chemical Sciences, Wyeth, CN 8000, Princeton, NJ 08543-8000, USA
[b] Albany Molecular Research, Albany, NY, USA
[c] Neuroscience, Wyeth, CN 8000, Princeton, NJ 08543-8000, USA
[d] Department of Chemical Sciences, Wyeth, 200 Cambridge Park Drive, Cambridge, MA 02140, USA

ARTICLE INFO

*Article history:*
Received 12 January 2010
Revised 14 February 2010
Accepted 18 February 2010
Available online 23 February 2010

*Keywords:*
Alzheimer's disease (AD)
BACE1 inhibitors
Beta-amyloid peptide (Aβ)
2-Aminopyridines

ABSTRACT

The proteolytic enzyme β-secretase (BACE1) plays a central role in the synthesis of the pathogenic β-amyloid in Alzheimer's disease. Recently, we reported small molecule acylguanidines as potent BACE1 inhibitors. However, many of these acylguanidines have a high polar surface area (e.g. as measured by the topological polar surface area or TPSA), which is unfavorable for crossing the blood–brain barrier. Herein, we describe the identification of the 2-aminopyridine moiety as a bioisosteric replacement of the acylguanidine moiety, which resulted in inhibitors with lower TPSA values and superior brain penetration. X-ray crystallographic studies indicated that the 2-aminopyridine moiety interacts directly with the catalytic aspartic acids Asp32 and Asp228 via a hydrogen-bonding network.



Alzheimer's disease (AD)[‡] is a progressive, degenerative disease of the brain and recognized as the leading cause of dementia in the aging population. The prognosis of AD is poor and there is a great need for medical intervention of this disease. Currently, the approved medical therapies consist of cholinesterase inhibitors and *N*-methyl D-aspartate (NMDA) antagonists, that reduce the symptomatology of the disease in the initial phase, but do not appear to be capable of curing or stopping its progression.[1,2] The pathological hallmarks of AD include the aggregation and extracellular deposition of β-amyloid peptide (Aβ), which leads to plaque formation, and the abnormal hyperphosphorylation of tau protein, which leads to the intracellular formation of neurofibrillary tangles.[3,4] β-amyloid deposits are predominately aggregates of the Aβ peptides (Aβ, 39–43 residues) resulting from the endoproteolysis of the amyloid precursor protein (APP).[5,6] These peptide fragments result from the sequential cleavage of APP, first at the N-terminus by β-secretase enzyme (β-site APP cleaving enzyme, BACE1),[7–13] followed at the C-terminus by one or more γ-secretase complexes (intramembrane aspartyl proteases),[10] as part of the β-amyloidogenic pathway. Although the cause of AD remains unknown, a large body of evidence is beginning to accumulate that highlights the central role of Aβ in the pathogenesis of the disease.[11–13] Thus, processes that limit Aβ production and deposition by preventing formation, inhibiting aggregation, and/or enhancing clearance may offer effective treatments for AD. Since β-secretase mediated cleavage of APP is the first and rate-limiting step of the amyloidogenic processing pathway, BACE1 inhibition is considered a prominent therapeutic target for treating AD by diminishing Aβ peptide formation in AD patients.

We report herein the design and synthesis of novel pyrrolyl 2-aminopyridines as BACE1 inhibitors. This work is an extension of our previously reported acylguanidines BACE1 inhibitors[14] **1**. The acylguanidine inhibitors are polar compounds, particularly due to the acylguanidine moiety, as suggested by the high total polar surface area (TPSA), which we hypothesized was leading to the observed poor blood–brain barrier permeation (<5%). The objective of our studies is to modify the acylguanidine moiety, effectively reduce TPSA and thus improve compound permeability. Molecular modeling studies have suggested that the aminopyridine moiety (**2**; Fig. 1) could replace the acylguanidine moiety, bind satisfacto-

* Corresponding author.
*E-mail address:* malamas.michael@gmail.com (M.S. Malamas).
† Present address: Department of Computational and Structural Chemistry, GlaxoSmithKline, 709 Swedeland Road, King of Prussia, PA 19406, USA.

‡ *Abbreviations.* AD, Alzheimer's disease; Aβ, beta-amyloid peptide, APP, β-amyloid precursor protein; BACE, β-site APP cleaving enzyme; FRET, fluorescence resonance energy transfer; ELISA, enzyme-linked immune sandwich assay; CHO, Chinese hamster ovary. Atomic coordinates of the BACE1 crystal structure with compounds **32** (3L3A) and **44** (3L38) have been deposited in the Protein Data Bank, Research Collaboratory for Structural Bioinformatics, Rutgers University, New Brunswick, New Jersey.

0960-894X/$ - see front matter © 2010 Elsevier Ltd. All rights reserved.
doi:10.1016/j.bmcl.2010.02.075

rily to the bis-aspartate warhead, and also decrease the TPSA of the molecule. Furthermore, potentiometric p$K_a$ measurements of a series of acylguanidines and related analogs (unpublished data) suggested that the ideal p$K_a$ range for the acylguanidine mimetic would be 6–7, making 2-aminopyridine (p$K_a$ = 6.86) within the appropriate range. Recently, aminoheterocycles as BACE1 inhibitor have also been disclosed.[15] The synthesis and SAR evaluation of the aminopyridines as BACE1 inhibitors will be the central focus of this paper. The X-ray crystallographic studies of the aminopyridines complexed with the BACE1 enzyme, which showed that the 2-aminopyridine moiety directly interacts with the catalytic aspartic acids Asp32 and Asp228 via a hydrogen-bonding network as intended, will also be discussed.

The compounds needed to delineate the SAR for this study were prepared according to synthetic Schemes 1 and 3[19]. The 1,4-diarylbutane-1,4-diones (**5**; Scheme 1) were prepared according to Kulinkovich's synthetic protocol[18] in a one-step cross coupling-reaction of ketones **3** and **4** in the presence of $ZnCl_2$. These diketones were treated with amines **6** and **7** to produce the corresponding pyrroles **8** and **11**, respectively. Demethylation of pyrrole **8** with boron tribromide furnished phenol **9**, which upon treatment with cesium carbonate and alkyl iodides produced alternately substituted ethers **10**. Alkyl-hydroxyl analogs **12** and **13** were prepared by two different synthetic routes from the common pyrrole intermediate **11**. In route a, pyrrole **11** was first treated with ethanolamine and subsequently with iron metal to furnish aminopyridines **12** (X = NH). In route b, the initial demethylation of the methoxy group of **11** was followed by alkylation and reduction with iron metal to produce aminopyridines **13** (X = O-alkyl). The required starting amines for these assemblies, **6** and **7** were prepared according to Scheme 2. Treatment of amino-pyridine **14** with phthalic anhydride produced imide **15**, which was brominated to furnish benzyl bromide **16**. Reaction of **16** with potassium

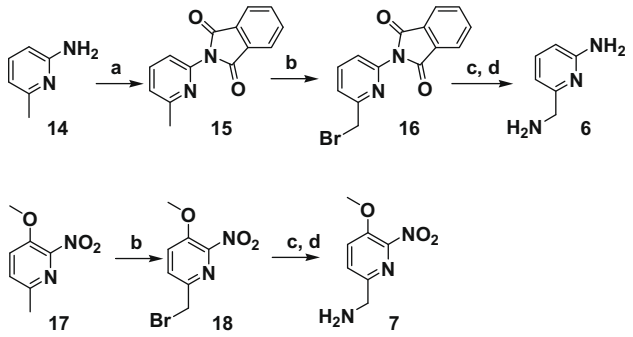


**Scheme 2.** Reagents: (a) phthalic anhydride, AcOH; (b) NBS AIBN, $CCl_4$; (c) potassium phthalimide; (d) hydrazine, EtOH.

phthalimide and subsequent hydrolysis with hydrazine furnished amine **6**. Amine **7** was prepared in a similar process as that of **6** starting from pyridine **17**. The 5-oxo-pyrimidinyl analogs **22** and ethanolamines **23** were prepared according to Scheme 3, from ketones **20** and **21**. Ketone **20** was prepared from 4-fluoroacetophenone **19** upon treatment with 5-hydroxyl pyrimidine. Amides **26** were prepared from **24** (prepared according to Kulinkovich's synthetic protocol[18]) by initially generating the acyl chloride that then followed by amide formation and cyclization to pyrrole as described in Scheme 1.

We have previously reported[14] the SAR studies of the acylguanidine series **1**, where the initial HTS hit **1** was rapidly optimized by using structure-based drug design techniques. While this class of inhibitors demonstrated excellent potency for the BACE1 enzyme ($IC_{50}$ ~50 nM), we felt that the polar nature of the acylguanidine moiety may have affected their permeability properties. As a

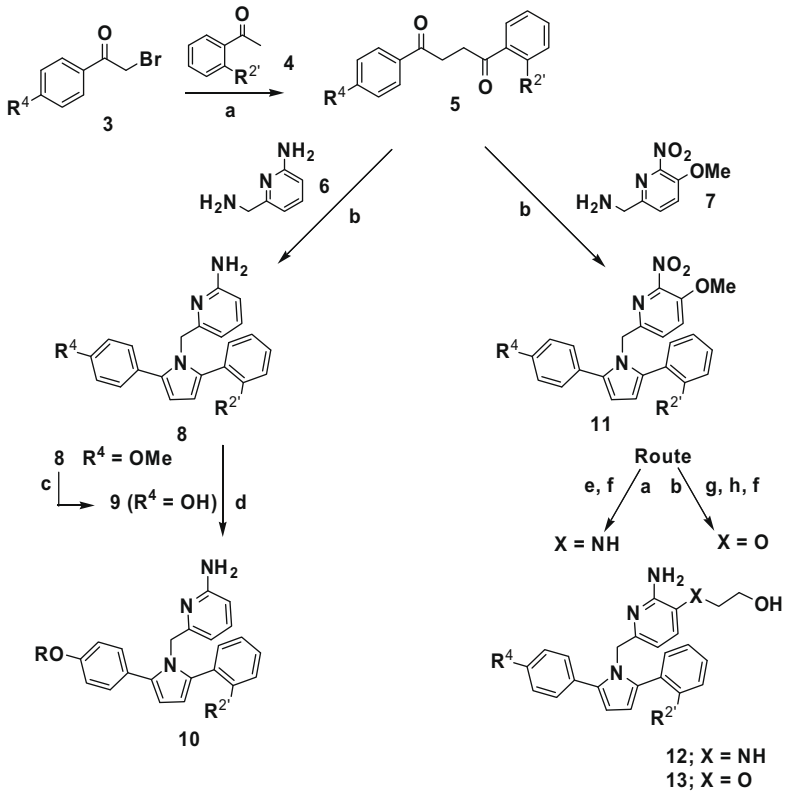


**Scheme 1.** Reagents: (a) $ZnCl_2$, $Et_3N$, *t*-BuOH; (b) *p*-TsOH, toluene, EtOH; (c) $BBr_3$, $CH_2Cl_2$; (d) RI, $Cs_2CO_3$, actetone; (e) ethanolamine, water, EtOH; (f) Fe, $NH_4Cl$, MeOH, water; (g) LiCl, DMF; (h) $BrCH_2CH_2OH$, $K_2CO_3$, DMSO.

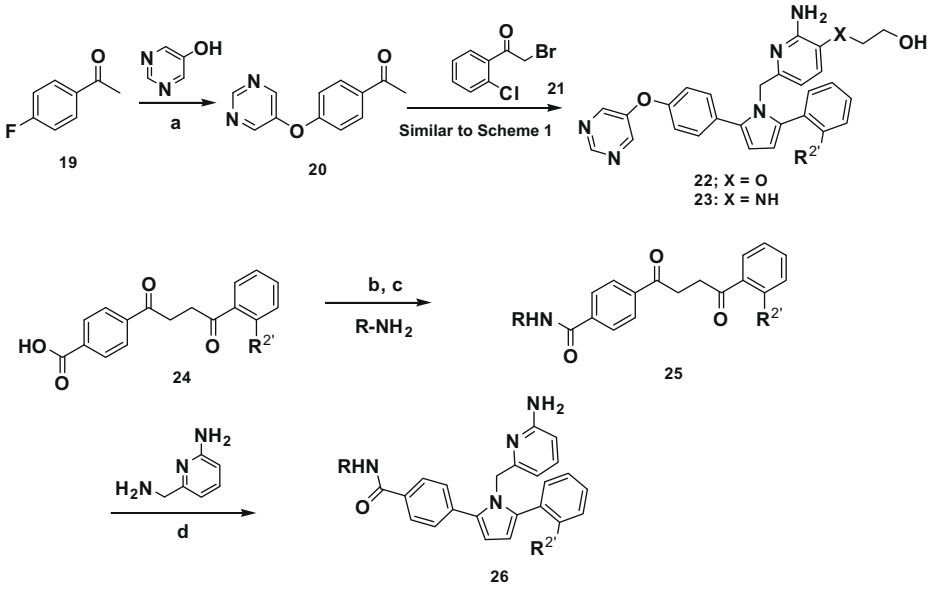


**Scheme 3.** Reagents: (a) $K_2CO_3$, DMAC; (b) $SOCl_2$; (c) $Et_3N$, THF; (d) *p*-TsOH, toluene, EtOH.

result the acylguanidines have demonstrated poor blood–brain barrier permeability (<5%) in addition to weak inhibition in an ELISA cell-based assay ($EC_{50}$ >1 μM). As mentioned earlier, our objective was to identify a less polar bioisosteric replacement of the acylguanidine moiety with improved physicochemical properties. Toward this end, we have employed modeling and X-ray studies and have discovered that the aminopyridine nucleus can successfully replace the acylguanidine moiety with comparable potency (**2** vs **1**; Fig. 1). These new aminopyridine inhibitors, in general, have reduced polar surface area (as measured by TPSA) relative to the analogous acylguanidines (i.e., TPSA values 44 vs 86 for **2** vs **1**). As expected, modulating this physicochemical parameter has enhanced the brain permeability of compound **2**, which showed an excellent central drug exposure with a brain to plasma ratio of 1.7, compared to 0.04 of compound **1**. Having accomplished our initial objective by effectively replacing the polar acylguanidine moiety with the aminopyridine group, next, we focused the SAR studies on further improving the potency of this new class of compounds. As can be seen, the docking of ligand **2** to the X-ray crystal structure of the acylguanidine **1** bound to BACE1 (Fig. 2) has generated a nearly perfect superimposition of these two ligands. The docking exercise further suggests that building off the *para*-position of the phenyl moiety occupying the S1-pocket would allow for projection directly towards the unoccupied S3 region. Following a similar SAR approach as we have disclosed with the acylguanidines,[14] we were able to improve the potency of target compound **2**. To that end, introduction of alkoxy groups (Table 1, entries **28**–**32**) at the *para*-position of the P1 phenyl

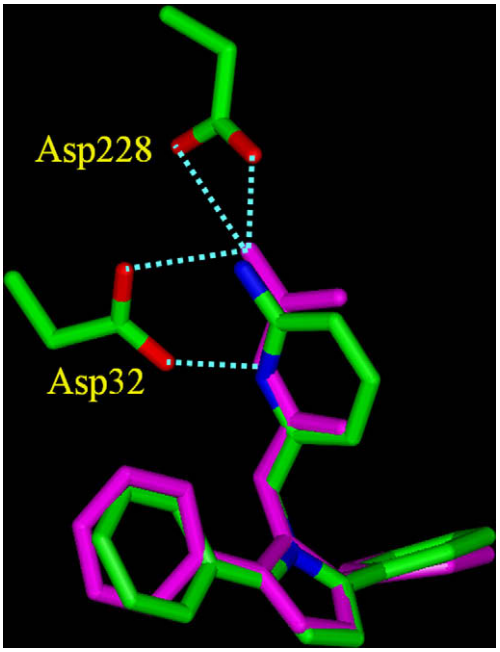


**Figure 2.** Crystal structure of BACE1 complexed with **1** (shown in magenta) and **2** (shown in green) are overlayed. Key hydrogen-bonding interactions between ligand **1** and the protein's catalytic aspartic acids Asp32 and Asp228 are highlighted with blue dashed lines. Aminopyridine **2** superimposes almost perfectly with acylguanidine **1**.

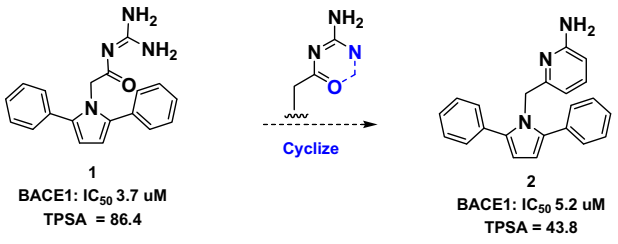


**Figure 1.** Bioisosteric replacement of the acylguanidine moiety.

resulted in an approximate 10-fold potency increase (**30**, **32** vs **2**). While the five-carbon chain analogs **30** produced the most active compound, both the shorter chained (entries **28**–**29**) and longer chained-analogs (entry **31**) were less potent. The three-carbon nitrile analog **32** was similar to **30** in potency. As shown below in the X-ray structure of **32** complexed with BACE1, the nitrile group of **32** extends deep into S3 pocket, thus contributing to the ligand affinity. Introduction of linear chain amides (entries **33**–**36**) at the *para*-position of the P1 phenyl have produced variable results. Allyl-amide **36** was 10-fold better than **2**, while the satu-

**Table 1**
Pyrrolyl 2-aminopyridines

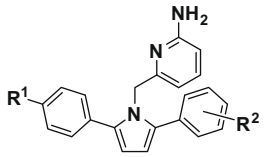


| Compd | $R^1$ | $R^2$ | BACE1 $IC_{50}$ μM | BACE2 % Inh. 12.5 μM | Cathepsin D % Inh. 12.5 μM | ELISA $EC_{50}$ μM |
|---|---|---|---|---|---|---|
| **2** | H | H | 5.2 ± 1.4[a] | 15 | 5 | 15.4 ± 0.9[a] |
| **27** | OMe | 2-Cl | 2.45 | 30 | 12 | 16 ± 1.7 |
| **28** | $O(CH_2)_2CH_3$ | 2-Cl | 1.15 | 48 | 7 | IA |
| **29** | $O(CH_2)_3CH_3$ | 2-Cl | 1.65 | 31 | 6 | IA |
| **30** | $O(CH_2)_4CH_3$ | 2-Cl | 0.55 ± 0.1 | 31 | 6 | 2.1 ± 0.4 |
| **31** | $O(CH_2)_5CH_3$ | 2-Cl | 45% @ 12.5 μM | 13 | 0 | IA |
| **32** | $O(CH_2)_3CN$ | 2-Cl | 0.42 | $IC_{50}$ = 7.1 μM | 26 | 5.2 ± 0.9 |
| **33** | $C(=O)NHCH_2CH_3$ | H | 2.25 | 36 | 9 | IA |
| **34** | $C(=O)NH(CH_2)_2CH_3$ | H | 3.0 | 28 | $IC_{50}$ = 44 .3 μM | IA |
| **35** | $C(=O)NH(CH_2)_3CH_3$ | H | 3.0 | 45 | 0 | nt |
| **36** | C(=O)NH-allyl | H | 0.59 | 6.2 | $IC_{50}$ = 43.6 μM | 4.8 ± 1.5 |
| **37** | $C(=O)NH–CH(CH_3)_2$ | H | 1.78 | 6.58 | 0 | IA |
| **38** | C(=O)NH-cyclopropane | H | 1.2 | 10.6 | 13 | IA |
| **39** | C(=O)NH-cyclobutane | H | 3.4 | 38.4 | 42.1 | IA |
| **40** | O-Ph | 2-Cl | 0.85 ± 0.2 | 16 | 0 | 9.2 ± 1.5 |
| **41** | *O*-4-Pyridyl | 2-Cl | 0.59 | 7.22 | 6 | 4.8 ± 1.2 |
| **42** | *O*-3-Pyridyl | 2-Cl | 0.41 ± 0.2 | 7.1 ± 0.07 | 27 | IA |
| **43** | *O*-2-Pyridyl | 2-Cl | 0.81 | 6.61 | 16 | IA |
| **44** | *O*-5-Pyrimidinyl | 2-Cl | 0.1 ± 0.02 | 9.7 ± 0.8 | 16 | 2.2 ± 0.5 |
| **45** | *O*-2-Pyrazinyl | 2-Cl | 0.46 | 46.6 | 3 | 13.3 ± 1.2 |
| **46** | *O*-2-Pyridazinyl | 2-Cl | 0.41 | 10.4 | 4 | IA |
| **47** | *O*-2-Thiazole | 2-Cl | 0.29 | 3.4 | 0 | 11.8 ± 0.2 |
| **48** | NH-5-Pyrimidinyl | 2-Cl | 0.98 | 9.8 | 32 | 8.6 ± 1.7 |

[a] $IC_{50}$ and $EC_{50}$ values are the means of at least two experiments ± SD. Values without SD are for a single determination only.

rated alkyl amides (**33**–**35**) were only marginally improved. The bulkier isopropyl- (**37**) and cycloalkyl-amides **38** and **39** were also slightly better than **2**.

Furthermore, to better fill the S3 region of the pocket, we have explored aromatic groups (**40**–**48**) linked at the *para*-position of the P1 phenyl with either an oxygen or a nitrogen atom. Despite the increased substituent size, most aromatic analogs were about 5–10-fold more potent than the parent compound **2**, with the notable example being the pyrimidinyl analog **44** which was the most potent compound with an $IC_{50}$ value of 100 nM for BACE1. Similarly to the parent compound **2**, aminopyridine **44** also demonstrated high brain permeability with a brain to plasma ratio of 1.1, despite an increase of the compound's total polar surface area (TPSA = 79).

To further validate our modeling calculations, **44** was then co-crystallized with the BACE1 enzyme, and as shown in Figure 3,

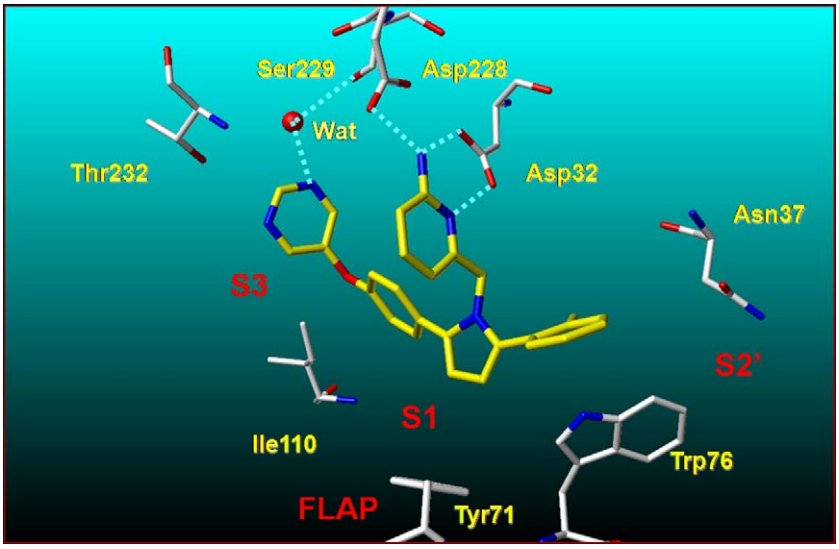


**Figure 3.** Crystal structure of BACE1 complexed with **44**. Key hydrogen-bonding interactions between ligand and protein at the catalytic aspartic acids Asp32 and Asp228, and the S3 conserved water are highlighted with blue dashed lines.

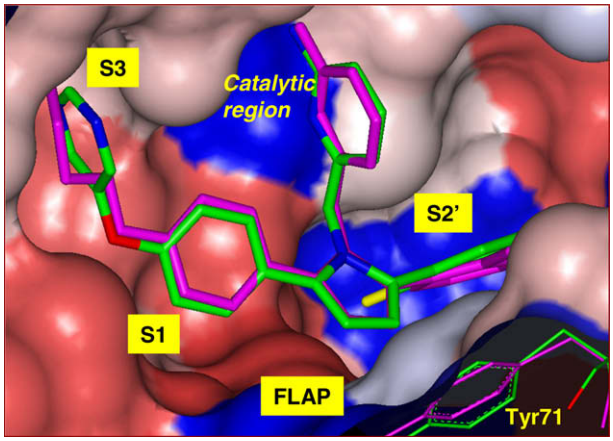


**Figure 4.** Crystal structures of BACE1 complexed with **32** (magenta) and **44** (shown in green) are overlayed. Substituents at the *para*-position of the P1 phenyl project deep into S3 pocket. The aminopyridine moiety orients toward the catalytic region of the enzyme and the pyrrole ring of the ligand points toward the FLAP region, making a π-edge stacking interaction with Tyr71.

the pyrimidine moiety projects deep into S3 pocket and makes a water-bridge contact with Ser229 through the buried conserved water found near the catalytic site of the enzyme. This water-bridge contact together with the additional van der Walls contacts between the ligand and enzyme backbone at the S3 region are consistent with the ligand's increased potency. In addition, the crystal structure shows that both the amino group and the pyridine nitrogen of the aminopyridine moiety make direct contacts with the catalytic aspartic acids Asp32 and Asp228 via a hydrogen-bonding network as expected. Finally the P1 and P2′ phenyls make van der Waals interactions at the S1 and S2′ pockets, while the pyrrole ring of the ligand points toward the FLAP region, presumably making a π-edge stacking interaction with Tyr71.

In order to confirm the orientation of the alkyl chain of the ligands that bear such a group at the *para*-position of the P1 phenyl, analog **32** was also co-crystallized with BACE1. The examination of the BACE1:**32** structure overlayed with **44** (Fig. 4) revealed both molecules superimpose very well and the alkyl chain of **32** orients similar to the aromatic group of **44**, extending deep into the S3 pocket.

Concomitant with these investigations, we explored analogs that would be able to access the S1′ region and potentially improve potency further. Taking into account the findings of the acylguanidine's series[14] and using molecular modeling techniques, we have identified the potential of adding substituents at position-3 of the aminopyridine moiety to extend deep into the S1′ region and improve ligand affinity. Additionally, the S1′ region differs in size and relative hydrophobicity compared to other aspartyl proteases, and thus affords an opportunity to improve the ligand selectivity. Based on precedents from our previous SAR work with the acylguanidines,[14,16,17] we have introduced alkyl-hydroxyl groups at position-3 of the aminopyridine moiety (Table 2, entries **49**–**54**), which resulted in enhancement of ligand potency. The oxo-ethyl-hydroxyl analog **49** was about 10-fold more potent than the lengthier propyl-hydroxyl analog **50**. In contrast to this finding, the analogous amino-alcohols **51** and **52** showed similar potency. Next, we introduced the ethyl-hydroxyl group to the previously optimized pyrimidinyl analog **44**, and this combination has resulted in the most potent compounds of this series. Analogs **53** and **54** exhibited $IC_{50}$ values of 40 and 70 nM, respectively, for BACE1. To our satisfaction, their cell-based activity also tracked well with their increased molecular binding. Not surprising, the introduction of the alkyl alcohols have resulted in an increase of the TPSA value of the molecule (TPSA >90) with the expected decrease in overall brain permeability (brain to plasma ratio ~0.25). Efforts to further improve the potency of this class of BACE1 inhibitors without affecting the molecular polarity (TPSA, etc.) and brain permeability will be the subject of a later disclosure.

The aminopyridine inhibitors were also evaluated against BACE2 and cathepsin D. The BACE2 selectivity ranged between 10–130-fold, while they were even more selective against cathepsin D (>100-fold), with the most potent inhibitor **53** ($IC_{50}$ = 40 nM) showing >100-fold selectivity against BACE2, and >500-fold against cathepsin D.

In summary, we have described the discovery of the 2-aminopyridine moiety as a bioisosteric replacement of the acylguanidine moiety with lower TPSA values and superior brain penetration. Several analogs have shown low nanomolar potency and >100-fold selectivity against BACE2 and cathepsin D. X-ray crystallographic studies indicated that the 2-aminopyridine moiety interacts directly with the catalytic aspartic acids Asp32 and Asp228 via a hydrogen-bonding network. Key substitutions at the P1 phenyl and the aminopyridine moiety of the ligand, extend deep into S3 and S1′ regions enhancing the ligand's affinity.

**Table 2**
Substituted aminopyridines

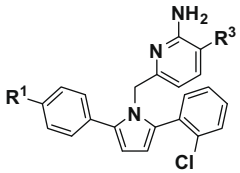


| Compd | $R^1$ | $R^3$ | BACE1 $IC_{50}$ μM | BACE2 % Inh. 12.5 μM | Cathepsin D % Inh. 12.5 μM | ELISA $EC_{50}$ μM |
|---|---|---|---|---|---|---|
| **49** | $O(CH_2)_4CH_3$ | $O(CH_2)_2OH$ | 0.11[a] | 1.7 | 4 | 13.6 ± 2.1[a] |
| **50** | $O(CH_2)_4CH_3$ | $O(CH_2)_3OH$ | 46% @ 1 μM | 47 | 0 | IA |
| **51** | $O(CH_2)_4CH_3$ | $NH(CH_2)_2OH$ | 0.17 | $IC_{50}$ = 1.0 | 43 | 3.2 ± 0.8 |
| **52** | $O(CH_2)_4CH_3$ | $NH(CH_2)_3OH$ | 0.22 | $IC_{50}$ = 0.47 | $IC_{50}$ = 7.2 ± 0.9 | IA |
| **53** | *O*-5-Pyrimidinyl | $O(CH_2)_2OH$ | 0.04 ± 0.01 | 5.43 | 23 | 0.44 ± 0.04 |
| **54** | *O*-5-Pyrimidinyl | $NH(CH_2)_2OH$ | 0.07 | 8.46 | 31 | 0.19 ± 0.04 |

[a] $IC_{50}$ and $EC_{50}$ values are the means of at least two experiments ± SD. Values without SD are for a single determination only.

## References and notes


1. Enz, A.; Amstutz, R.; Boddeke, H.; Gmelin, G.; Malanowski, J. *Am. J. Geriatr. Pharmacother.* **2005**, *3*, 39.
2. Arendt, T. *Neuroscience* **2001**, *102*, 723.
3. Dickson, D. W. *J. Neuropathol. Exp. Neurol.* **1997**, *56*, 321.
4. (a) Selkoe, D. J. *Science* **1997**, *275*, 630; (b) Hardy, J.; Selkoe, D. J. *Science* **2002**, *297*, 353.
5. Vassar, R.; Citron, M. *Neuron* **2000**, *27*, 416.
6. Selkoe, D. J. *Physiol. Rev.* **2001**, *81*, 741.
7. Hussain, I.; Powell, D.; Howlett, D. R.; Tew, T. G.; Meek, T. D.; Chapman, C.; Gloger, I. S.; Murphy, K. E.; Southan, C. D.; Ryan, D. M.; Smith, T. S.; Simmons, D. L.; Walsh, F. S.; Dingwall, C.; Christie, G. *Mol. Cell Neurosci.* **1999**, *14*, 419.
8. Lin, X.; Koelsch, G.; Wu, S.; Downs, D.; Dashti, A.; Tang, J. *Proc. Natl. Acad. Sci. U.S.A.* **2000**, *97*, 1456.
9. Sinsa, S.; Anderson, J. P.; Barbour, R.; Basi, G. S.; Caccavello, R.; Davis, D.; Doan, M.; Dovey, H. F.; Frigon, N.; Hong, J.; Jacobson-Croak, K.; Jewett, N.; Keim, P.; Knops, J.; Lieberburg, I.; Power, M.; Tan, H.; Tatsuno, J.; Tung, J.; Schenk, D.; Seubert, P.; Suomensaari, S. M.; Wang, S.; Walker, D.; Zhao, J.; McColongue, L.; John, V. *Nature* **1999**, *402*, 537.
10. Vassar, R.; Bennett, B. D.; Babu-Khan, S.; Kahn, S.; Mendiaz, E. A.; Denis, P.; Teplow, D. B.; Ross, S.; Amarante, P.; Loeloff, R.; Luo, Y.; Fischer, S.; Fuller, J.; Edenson, S.; Lile, J.; Jarosinski, M. A.; Biere, A. L.; Curran, E.; Burgess, T.; Louis, J.-C.; Collins, F.; Treanor, J.; Rogers, G.; Citron, M. *Science* **1999**, *286*, 735.
11. Selkoe, D. J. *Ann. Intern. Med.* **2004**, *140*, 627.
12. Alloul, K.; Sauriol, L.; Kennedy, W.; Laurier, C.; Tessier, G.; Novosel, S.; Contandriopoulos, A. *Arch. Gerontol. Geratr.* **1998**, *27*, 189.
13. (a) Enz, A.; Amstutz, R.; Boddeke, H.; Gmelin, G.; Malanowski, J. *Prog. Brain Res.* **1993**, *98*, 431; (b) Fillit, H.; Hill, J. *Am. J. Geriatr. Pharmacother.* **2005**, *3*, 39.
14. Cole, D. C.; Manas, E. S.; Stock, J. R.; Condon, J. S.; Jennings, L. D.; Aulabaugh, A.; Chopra, R.; Cowling, R.; Ellingboe, J. W.; Fan, K. Y.; Harrison, B. L.; Hu, Y.; Jacobsen, S.; Jin, G.; Lin, L.; Lovering, F. E.; Malamas, M. S.; Stahl, J.; Strand, J.; Sukhedo, M. N.; Svenson, K.; Turner, M. J.; Wagner, E.; Wu, J.; Zhou, P.; Bard, J. *J. Med. Chem.* **2006**, *49*, 6158.
15. Stachel, S.; Coburn, C.; Rush, D.; Jones, K.; Zhu, H.; Rajapakse, H.; Graham, S. L.; Simon, A.; Holloway, M. K.; Allison, T. J.; Munshi, S. K.; Espeseth, A. S.; Zuck, P.; Colussi, D.; Wolfe, A.; Pietrak, B. L.; Lai, M.; Vacca, J. *Bioorg. Med. Chem. Lett.* **2009**, *19*, 2977.
16. Cole, D.; Stock, J.; Chopra, R.; Cowling, R.; Ellingboe, J.; Fan, K.; Harrison, B.; Hu, Y.; Jacobsen, S.; Jennings, L.; Jin, G.; Lohse, P.; Malamas, M. S.; Manas, E.; Moore, W.; O'Donnell, M.; Olland, A.; Robichaud, A.; Svenson, K.; Wu, J.; Wagner, E.; Bard, J. *Bioorg. Med. Chem. Lett.* **2008**, *18*, 1063.
17. Jennings, L.; Cole, D.; Stock, J.; Sukhdeo, M.; Ellingboe, J.; Cowling, R.; Jin, G.; Manas, E.; Fan, K.; Malamas, M. S.; Harrison, B.; Jacobsen, S.; Chopra, R.; Lohse, P.; Moore, W.; O'Donnell, M.; Hu, Y.; Robichaud, A.; Turner, J.; Wagner, E.; Jonathan Bard *Bioorg. Med. Chem. Lett.* **2008**, *18*, 767.
18. Nevar, N. M.; Kelin, A. V.; Kulinkovich, O. G. *Synthesis* **2000**, 1259.
19. Detailed experimental of the preparation of the compounds described in this Letter are reported in US Patent 0173049, 2006.